Available online at www.sciencedirect.com

ScienceDirect

Procedia Engineering 119 (2015) 1338 – 1347

Procedia Engineering

www.elsevier.com/locate/procedia

13th Computer Control for Water Industry Conference, CCWI 2015

Interface model between the bioreactor and the membrane in a membrane bioreactor for wastewater treatment.

Tomasz Janus*, Bogumil Ulanicki

Water Software Systems, De Montfort University, The Gateway, LE1 9BH, Leicester, United Kingdom

Abstract

This paper proposes a structure of an integrated mathematical model of a membrane bioreactor (MBR) and describes the links between two main parts of a MBR model: the bioreactor and the membrane. In case of an immersed MBR three types of links are considered: a relationship between specific cake resistance (SCR) and extracellular polymeric substances (EPS) in the bioreactor, a relationship between air scour rate and shear stresses on the membrane surface, and a relationship between concentration of soluble microbial products (SMP) in the bioreactor and rate of pore constriction. While SMP concentration features directly in the equations of pore constriction, EPS are assumed to affect SCR which in turn has an effect on cake filtration. The relationship between EPS and SCR is described with a linear algebraic equation. Shear stresses on the membrane surface are calculated as a function of air scour rate with a one-dimensional slug flow model.

Peer-review under responsibility of the Scientific Committee of CCWI 2015

Keywords: activated sludge model, MBR, SMP, EPS

1. Introduction

MBR systems are widely applied in municipal and industrial wastewater treatment. The main three reasons for their popularity are: tightening effluent discharge standards, rising water scarcity, and limited land availability for expansion of existing wastewater treatment plants (WWTPs). Under such circumstances MBRs outperform traditional treatment systems thanks to superior effluent quality, better process stability and smaller footprint. Despite of the widespread use of MBRs in wastewater treatment this technology is currently missing bespoke dynamic process models that would allow simulation of MBR-based plants in commercial WWTP simulation packages along with conventional processes such as activated sludge reactors, trickling filters, or sedimentation tanks. To circumvent this shortcoming MBRs are often modelled as a conventional activated sludge process (CASP), albeit with a higher mixed liquor suspended solids (MLSS) concentration and with ideal clarification replacing membrane filtration. This approach was successful on numerous occasions in predicting sludge production, oxygen demand and effluent concentrations of such compounds as ammoniacal nitrogen or nitrates in MBR systems [1] but it does not allow us to calculate the costs associated with the membrane filtration unit as it neglects the impact of fouling on the overall operating costs and the

* Corresponding author. Tel.: +44-116-257-7070.
E-mail address: tjanus@dmu.ac.uk

Peer-review under responsibility of the Scientific Committee of CCWI 2015
doi:10.1016/j.proeng.2015.08.973

role of biopolymers in fouling. Until now only a handful of bespoke dynamic mathematical models for membrane bioreactors have been described in scientific literature although, as will be briefly outlined below, recent years have seen some important developments in modelling of MBR systems. The most recent published work on modelling MBRs with full activated sludge model (ASM) models coupled with membrane fouling is briefly described below.

Zarragoitia-González et al.[2] linked an activated sludge model of Lu et al.[3] with a comprehensive membrane fouling model of Li and Wang[4] where fouling is assumed to be the product of pore constriction, sludge cake accumulation, and dynamic film layer formation. Bella et al.[5] connected a ASM1-based model with SMP kinetics closely resembling that of Lu et al.[3] with a membrane fouling model based on the model of Lee et al.[6]. Unfortunately, the study was primarily focussed on predicting effluent chemical oxygen demand (COD) whilst the effects of SMP production on irreversible fouling were not modelled. Additionally, in both publications the Petersen matrices of the biological models violate the mass and charge conservation equations. Mannina et al.[7] improved the model of Bella et al.[5] by swapping the non-mass and charge conserving model of Lu et al.[3] with a modified Activated Sludge Model No. 1 (ASM1) implementing the SMP kinetics introduced by Jiang et al.[8]. The membrane filtration model was modified to include more fouling mechanisms whilst keeping the sectional model approach of Lee et al.[6] and the deep bed filtration equations introduced originally by Bella et al.[5]. Although their model was found to be in a good agreement with the measurements obtained from a MBR pilot plant, it assumes that SMP only affects SCR whilst neglecting the effects of SMP on pore constrictions. Most recently Suh et al.[9] developed an integrated MBR model based on the benchmark simulation layout of Maere et al.[10], the combined EPS and SMP production ASM3-based model of Janus and Ulanicki[11] and the fouling model of Li and Wang[4]. Unfortunately, similarly to the above mentioned models, no functional relationships between SMP and irreversible fouling have been provided. In addition to these original research papers a number of review articles and general publications on MBR modelling have appeared in recent years, such as the short review of modelling studies on membrane bioreactors by Ng and Kim[12], the comprehensive review of the applications of activated sludge models in MBR simulation studies by Fenu et al.[1], the review papers on integration of biological and filtration models by Zuthi et al.[13], Naessens et al.[14], Naessens et al.[15] and a PhD thesis of Janus[16].

The above short literature review tells us that despite of the urging need for a dynamic mathematical model of a MBR reactor all of the models proposed up to date have their shortcomings. This is due to a multitude of factors. First, the fidelity of biological and fouling models is still questionable with regards to production of biopolymers, especially under dynamically changing conditions (see Janus[17],Janus and Ulanicki[18]) and mathematical description of fouling mechanisms, especially, with respect to MBRs- biofouling. Second, the relationships between both parts of the MBR system, i.e. the bioreactor and the membrane are, to a large extent, unknown. It is still uncertain whether SMP are a major foulant, what role floc size distribution (FSD) plays on membrane fouling, how SMP retention on the membrane depends indirectly on the operating conditions of the bioreactor and, directly, on its molecular weight distribution (MWD). Lastly, the flow patterns and the resulting shear stresses on the membrane surface during air-scouring are still in early research stage. This paper proposes a model structure which allows simulation of MBR systems taking into account some of the most important interactions between the biological and filtration parts of an MBR. Secondly, it focusses on these interactions, dependence of cake detachment on the air-scouring intensity and the link between EPS concentrations and SCR. These interactions are represented in the interface subsystem shown in Figure 1 on page 4.

2. Integrated model structure

The model was divided into three separate subsystems (see Figure 1): the Bioreactor (Subsystem 1), the Membrane (Subsystem 2) and the Interface (Subsystem 3). Subsystem 1 is described with a ASM-based biological model considering the kinetics of both soluble and bound polymers, contrary to the majority of biological models used in earlier studies which considered only the soluble biopolymer kinetics. Subsystem 2 describes membrane fouling and considers the role of both soluble and insoluble biopolymers on reversible and irreversible fouling, contrary to the previously published models which generally only consider the role of SMP in cake filtration (reversible fouling) rather than pore constriction (irreversible fouling), whilst neglecting the effects of EPS on fouling in general. The model structure assumes that irreversible fouling is caused by SMP whilst reversible fouling is accelerated by EPS content in MLSS which increases the specific cake resistance. Subsystem 3 links Subsystem 1 and Subsystem 2 by providing

a functional relationship between cake detachment rate in Subsystem 2 and air-scour intensity in Subsystem 1 as well as the relationship between SCR used as a parameter in the fouling model (Subsystem 2) and the EPS content in the activated sludge (Subsystem 1). Cake detachment is described as a function of air-scour rate with a formula obtained from the results of a steady-state slug flow model of Zaisha and Dukler[19] solved on the hollow fibre (HF) membrane module geometry of Busch et al.[20]. SCR is calculated as a function of EPS content with a modified formula of Ahmed et al.[21].

Subsystem 1 is described with a ASM1-based activated sludge model which additionally introduces three new states corresponding to the concentrations of, respectively, extracellular polymeric substances (EPS), utilisation associated products (UAP), and biomass associated products (BAP). For a thorough description of this model the reader is referred to Janus and Ulanicki[18]. Membrane fouling (Subsystem 2) is described with a modified version of a fouling model published by Liang et al.[22]. The model is based on two ordinary differential equations (ODEs) describing the rates of change in membrane resistance due to, respectively, reversible fouling associated with cake formation and irreversible fouling associated with pore constriction. More in-depth information about the model can be found in Janus and Ulanicki[23]. Both parts of the MBR system, i.e. the bioreactor and the membrane are in interaction with one another. The bioreactor produces MLSS, SMP and EPS which all affect the overall rate of membrane fouling. The membrane, on the other hand, retains a fraction of SMP leading to a buildup of SMP in the bioreactor. It is hypothesised that SMP are solely responsible for irreversible fouling, MLSS are directly linked to the amount of cake depositing on the membrane surface, whereas EPS content in activated sludge affects the cake's SCR. The rate of cake formation is reduced by air scouring which promotes particle back-transport from the membrane surface and at the same time aerates the bulk liquid. The oxygen transfer rate is however hindered by suspended solids in the bulk liquid, i.e. MLSS which increase the overall bulk liquid viscosity and lead to an increased mean air bubble diameter [24]. Cake formation is also controlled by periodic backwashing.

The above interactions, e.g. air-scouring, backwashing, SMP retention and dependence of cake filtration properties on EPS, are represented by the interface subsystem, i.e. Subsystem 3. Cake detachment is modelled with the relationship of Nagaoka et al.[25]. The average shear stress in the cake detachment equation is calculated from two polynomials approximating the results of the slug-flow model of Zaisha and Dukler[19] solved on the membrane module geometry of Busch et al.[20]. Backwashing is modelled by periodic resetting of the initial condition in the cake deposition equation at the end of each filtration phase. SMP retention on the membrane is described with a non-dimensional coefficient f_r denoting the ratio of the number of SMP molecules retained by the membrane to the total number of SMP molecules coming into contact with the membrane. Specific cake resistance is assumed to be linearly dependent on the EPS content in activated sludge, as reported in Nuengjamnong et al.[26] and Ahmed et al.[21]. The actual oxygen transfer rate (AOTR) is calculated with standard aeration equations and with parameter values taken from Maere et al.[10].

The block diagram of the MBR model structure is shown in Figure 1. Subsystem 1 receives an input vector $u_1(t)$ associated with the influent flow and composition plus an output vector $y_4(t)$ associated with the retentate flow and composition whilst producing an output vector $y_1(t)$. Part of the retentate flow is diverted from the retentate recirculation loop and forms an output vector $y_5(t)$ associated with the waste activated sludge (WAS) stream. Its composition is equal to the composition of $y_4(t)$. The sub-vector $\tilde{y}_1(t) \subset y_1(t)$ is composed of the state variables of Subsystem 1 which cause membrane fouling: $\tilde{y}_1(t) = (S_{SMP}\ X_{EPS}\ X_{MLSS})^T$, where S_{SMP} (gCOD m^{-3}) denotes the concentration of soluble microbial products (SMP), X_{EPS} (gCOD m^{-3}) denotes the concentration of extracellular polymeric substances (EPS) and X_{MLSS} (g m^{-3}) is the concentration of mixed liquor suspended solids (MLSS). Subsystem 3 receives the signal $\tilde{y}_1(t)$ and the input vector $u_2(t) = \left(Q_{air}\ t_f\ t_b\right)^T$, where Q_{air} (Nm^3 s^{-1}) denotes the volumetric air flow rate, t_f (s) denotes the filtration cycle duration time and t_b (s) is the backwash cycle duration time. With this data it then calculates the fouling coefficients, the shear rate on the membrane surface, and the filtration and backwash control signals which form the output signal $y_2(t)$. Outputs from the bioreactor $y_1(t)$ and the interface $y_2(t)$ form the inputs to the Subsystem 2 which produces two output vectors: $y_3(t)$ associated with the permeate stream and $y_4(t)$ associated with the retentate stream. Subsystem 1 and Subsystem 2 receive two external disturbance vectors, $w_1(t)$ and $w_2(t)$ which, in this case, consist of just one variable: the liquid temperature, T_l (^{o}C).

Since MBRs are typically equipped with microfiltration (MF) and ultrafiltration (UF) membranes with molecular weight cut-offs (MWCOs) above 10 kDa, all mono- and multivalent ions pass entirely across the membrane whilst particulate components are fully retained. Additionally, we assume that inert soluble and readily biodegradable or-

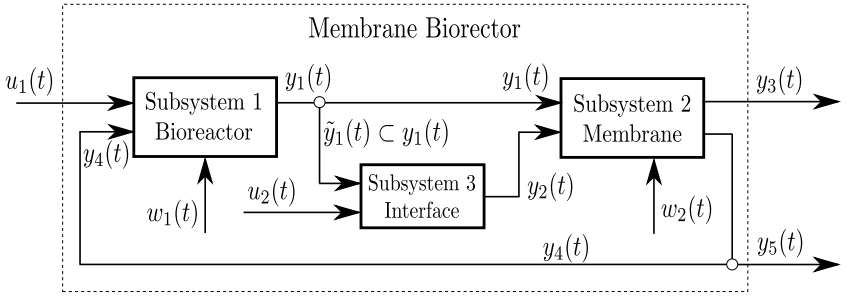

Fig. 1: Membrane Bioreactor model structure.

ganic compounds, and soluble organic nitrogen also entirely pass across the membrane. Since the data about retention of these substances on commercial UF membranes are hardly available and while bulk liquid concentrations of these substances in the downstream compartments of MBRs are small anyhow, this assumption is fully justified. Therefore, concentrations of all soluble components in $y_3(t)$ are equal to the respective bulk liquid concentrations in the last section of the membrane reactor whilst concentrations of all particulate components in $y_3(t)$ are null. Concentrations of all particulate variables in $y_4(t)$ and $y_5(t)$ are calculated from the mass balance equation around the membrane and are equal to $X_j/(1-\eta_f)$ where X_j denotes the concentration of j-th particulate state variable in the vector of state variable concentrations and η_f is the permeate recovery parameter defined as a ratio of permeate to feed flow. Since SMP are partly retained by the membrane due to its complex molecular composition, permeate SMP concentration $S_{SMP,e} = f_{nr}\, S_{SMP}$ where f_{nr} (–) denotes a non-retainable SMP fraction. SMP concentration in the retentate is again calculated from the mass balance equation around the membrane: $S_{SMP}\,(1-\eta_f\, f_{nr})/(1-\eta_f)$.

3. Membrane air-scouring model

Cake buildup in immersed MBRs is controlled mainly through coarse bubble aeration, i.e. injection of air bubbles of $\sim 6-13$ mm in diameter at the bottom of the membrane modules. These air bubbles rise and coalesce to form larger bubbles, usually occupying most of available free space. Whilst flowing upwards in the vicinity of the membrane, the bubbles create shear stresses on the membrane surface, leading to cake detachment. Various researchers postulate that the amount of air introduced into membrane modules is such that the flow regime resembles that of slug flow whereas others claim that the flow is cap bubbly, thus in a transition region between bubbly and slug flow. Drews et al.[27], for example, showed through experiments and simulation that bubbles of larger diameters undergo deformations during an upward flow due to drag and, in consequence, become cap-like rather than spherical. As shall be shown later, results of the simulations carried out in this study support these findings. Under specific aeration demands per membrane area (SAD_m) normally applied in immersed membrane bioreactors (iMBRs), i.e. ~0.2–1.2 $Nm^3\ m^{-2}\ h^{-1}$, gas phase fractions in a membrane module are characteristic of bubbly and cap-bubbly flow rather than slug-flow. The predicted Taylor bubble lengths are very short in comparison to liquid slug lengths, which suggests formation of cap-like, short air bubbles.

Nevertheless, since motion of cap bubbles is not well understood and the models describing cap bubbly flow are not available, air-scouring is modelled here with a well established slug flow model of Zaisha and Dukler[19]. As the number of equations formulating the slug flow model is rather large, these equations are not provided in this paper and need to be found in Table 1 of the original manuscript of Zaisha and Dukler in which D becomes d_{slug}, where d_{slug} (m) denotes the diameter of liquid slugs and $U_{SG} = \dfrac{Q_{air}}{A_{mod}}$, where U_{SG} (cm s^{-1}) denotes the superficial gas velocity and A_{mod} (m^2) denotes the total free area of the membrane module. Additionally, the equations in the original publication of Zaisha and Dukler have been supplemented with Equation 9, listed further down in the text, which describes an empirical relationship between the superficial liquid velocity U_{SL} and the superficial gas velocity U_{SG} in a iMBR studied by Böhm et al.[28]. The model is simulated under a range of operating conditions defined in Table 1 using a non-linear least squares method for minimisation of residuals with the trust region reflective algorithm implemented in MATLAB® Optimization Toolbox™.

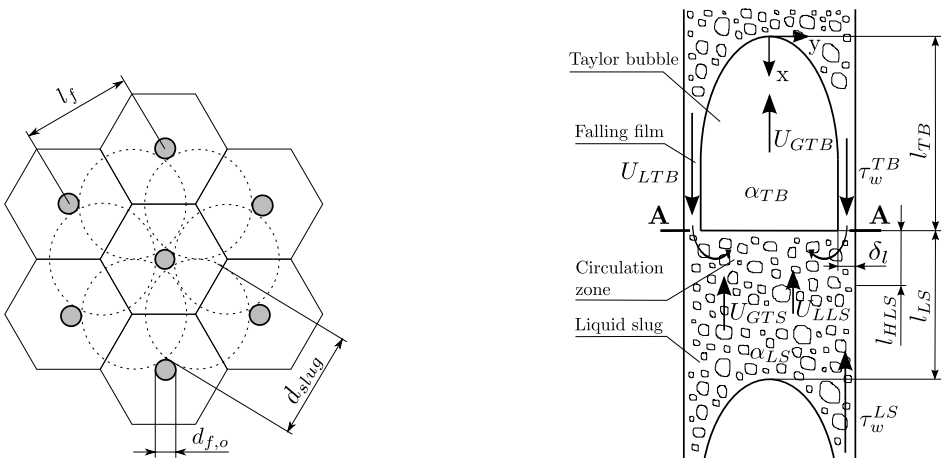

Fig. 2: (a) Hollow fibre module geometry in a horizontal cross-section adopted from Busch et al.[20] (b) Graphical representation of a slug flow problem - adopted from Zaisha and Dukler[19].

The computational domain for the slug flow model uses the hollow fibre module geometry of Busch et al.[20] shown in Figure 2a and described with Equations 1 - 4.

$$A_{hex} = \frac{\sqrt{3}\, {l_f}^2}{2} - \frac{\pi}{4}\, {d_{f,o}}^2 \tag{1}$$

$$A_{mod} = n_f\, A_{hex} \tag{2}$$

$$d_{slug} = \frac{2\, l_f}{\sqrt{3}} - d_{f,o} \tag{3}$$

$$A_{slug} = \pi \frac{d_{slug}^2}{4} \tag{4}$$

where A_{hex} (m^2) represents the hexagonal catchment area of a single fibre, l_f (m) is the distance between neighbouring fibres, $d_{f,o}$ (m) is the fibre's outer diameter, n_f (–) is the number of fibres in the module, d_{slug} (m) denotes the diameter of the liquid slugs, A_{slug} (m^2) is the cross-sectional (round) area of the liquid slugs and A_{mod} (m^2) is the total area of the membrane tank.

Among other variables the simulations return the values of liquid slug velocity, U_{LLS} (m s^{-1}) and falling liquid film thickness, δ_L (m) which are then used to calculate shear stresses caused by rising liquid slugs, τ_w^{LS} (Pa) and falling liquid film around the Taylor bubbles, τ_w^{TB} (Pa) with Equations 5-8 originally proposed by Busch et al.[20]. We are therefore able to calculate shear stresses on the membrane surface as a function of specific aeration demand per membrane area (SAD_m). τ_w^{LS} and τ_w^{TB} are averaged proportionally to the lengths of each section, i.e. liquid slug and Taylor bubble using the formula in Equation 5. The entire model for calculation of shear stresses is given below.

$$\tau_w = \beta \left|\tau_w^{TB}\right| + (1-\beta) \left|\tau_w^{LS}\right| \tag{5}$$

$$\tau_w^{LS} = \frac{\rho_L\, \lambda_{slug}\, (U_{LLS})^2}{8} \tag{6}$$

$$\lambda_{slug} = 0.316\, {Re_{cs}}^{-0.25} \tag{7}$$

$$\tau_w^{TB} = (\rho_L - \rho_G)\; g\; \delta_L \tag{8}$$

where τ_w (Pa) denotes the average shear stress on the fibre surface, β (–) denotes the length ratio of the Taylor bubble to the whole slug unit, λ_{slug} (–) is the coefficient in the Blasius' equation, Re_{cs} (–) is the Reynolds number based on the mean slug flow velocity and ρ_L and ρ_G (kg m^{-3}) are respectively liquid density and air density under normal

conditions. Rest of the equations used to describe slug flow in our membrane module is provided in Table 1 of the original manuscript of Zaisha and Dukler [19].

Although we may argue that absolute shear stress values $\left|\tau_w^{TB}\right|$ and $\left|\tau_w^{LS}\right|$ instead of the length-averaged and therefore time-averaged value τ_w are actually responsible for cake detachment, incorporation of τ_w^{TB} and τ_w^{LS} in the MBR model would require us to use a cake detachment model offering a more detailed description of cake detachment dynamics. Whilst the shear stresses caused by the falling liquid film (τ_w^{TB}) are much higher than shear stresses caused by rising liquid slugs (τ_w^{LS}), τ_w^{TB} should, in theory, be primarily responsible for cake detachment, but only if we disregarded the role of process dynamics. τ_w^{TB} occur on the membrane for very short periods of time due to the fact that air bubbles are very short in comparison to liquid slugs. Hence, although τ_w^{TB} are very large compared to τ_w^{LS}, the exposure time of cake to these shear stresses may not be sufficiently long to cause substantial cake detachment. Due to the lack of available information on cake detachment dynamics, τ_w^{TB} and τ_w^{LS} are averaged with respect of length (and hence time), using Equation 5. The time-averaged shear stress τ_w is then used as the input to the cake detachment model. Such an approach is also consistent with the rest of the slug-flow model which is formulated with static algebraic equations despite of a highly dynamic and chaotic characteristics of slug-flow. The slug-flow model used in this study is thus considered to give temporally and spatially averaged values for the parameters involved, in the same way as the highly fluctuating shear stresses are reduced in the model to a single time-averaged value.

An upward movement of air bubbles creates a velocity field and a density current leading to a circulating motion of bulk liquid in the membrane tank. The superficial liquid velocity, U_{SL} is hence induced by air flow and therefore depends on the superficial gas velocity, U_{SG}. This relationship depends on the tank and membrane module geometry, positioning and type of aeration devices, air bubble size, bulk liquid viscosity and other parameters. Since we only provide a simplified description of slug-flow whilst avoiding the use of Computational Fluid Dynamics (CFD) models, the velocity field inside the membrane tank is not calculated, but instead U_{SL} is linked to U_{SG} using a simple empirical modified equation of Chisti [28]. This relationship is very likely to be valid only for the system used by Böhm et al.[28] but since we do not work with a particular tank geometry, we can still use this relationship to demonstrate, in a qualitative manner, the overall effects of air scouring on the level of shear stresses on the membrane surface and ultimately, the rate of cake detachment.

$$U_{SL} = 47.12\, U_{SG}^2 - 6.624\, U_{SG} - 9.835 \times 10^{-2} \tag{9}$$

in which U_{SL} and U_{SG} are given in cm s^{-1}.

3.1. Air-scouring model results

Whilst the biological model and fouling models were calibrated on experimental data (see [18,23]), air scouring was investigated only from a theoretical point of view to provide a general insight into the air-water slug flow phenomenon in immersed HF membrane modules. Hence, the results, although qualitatively indicative, do not provide any accurate quantitative information. As already mentioned in the previous section, the model itself is a one-dimensional static simplification of a highly dynamic and often chaotic system and the relationship between U_{SL} and U_{SG} is of an empirical nature, hence the simulation results cannot be generalised. The model also does not take into account that majority of shear on the surface of the membrane fibres can be actually created by the fibres coming in contact with one another rather than air scouring. The sway is also not taken into account as the model assumes that the module geometry is invariant in time. Nevertheless, a simple theoretical analysis of aerated immersed membrane module hydraulics is still valuable as it provides an indication of the expected type of flow inside the module and the likely order of magnitude of shear stresses on the membrane surface.

The slug-flow model was simulated for a range of superficial gas velocities, U_{SG} between 1.0 and 5.0 m s^{-1} which satisfy aeration demands per membrane area (SAD_m) of 0.20 - 1.00 m^3 m^{-2} h^{-1}. All relevant inputs and parameters of the slug flow model are presented in Table 1.

The calculated average shear-stress values τ_w were found to form a third-order polynomial against U_{SG} and are approximated as such (see Equation 10, where each coefficient p_i is in a functional relationship with X_{MLSS} and T_l accordingly to Equation 11).

$$\tau_w(U_{SG}) = p_1\,(U_{SG})^3 + p_2\,(U_{SG})^2 + p_3\,(U_{SG}) + p_4 \tag{10}$$

Table 1: Values of the slug-flow model parameters adopted in the simulations.

Parameter	Description	Unit	Value
l_f	Distance between neighbouring fibres	m	0.01
$d_{f,o}$	Fibre's outer diameter	m	0.0025
h	Membrane module's (fibre's) height	m	1.8
A_{mod}	Module cross-section area	m^2	402.8
ρ_W	Density of water	kg m^{-3}	998.2
ρ_G	Density of air	kg m^{-3}	1.15
$\mu_{G,0}$	Dynamic gas viscosity under normal conditions	Pa · s	1.827×10^{-5}
$\sigma_{l,g}$	Surface tension between water and air	N m^{-1}	0.0729
U_{SG}	Superficial gas velocity	cm s^{-1}	1 – 5
X_{TSS}	Total Suspended Solids	kg m^{-3}	6, 13, 20
T_l	Bulk liquid temperature	^{o}C	8, 14, 20

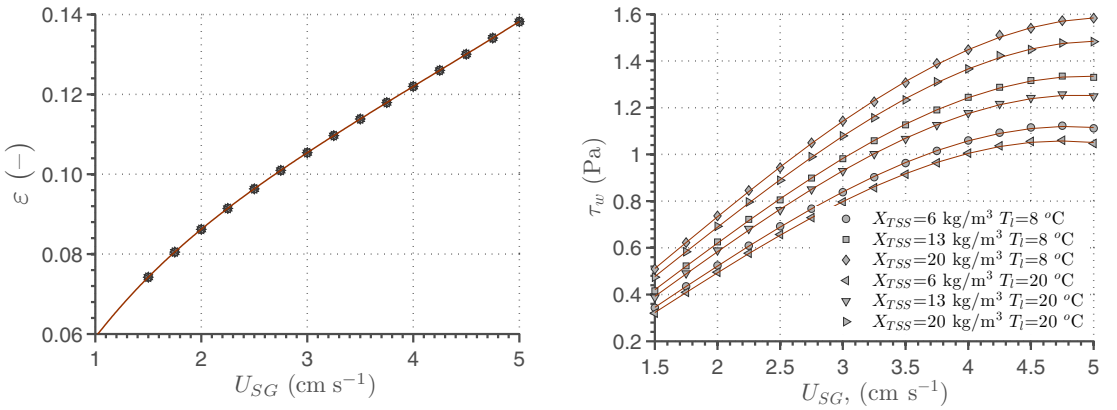

(a) (b)

Fig. 3: Gas fractions (a) and average shear stresses on the fibre surface (b) at different superficial gas velocities (U_{SG}), suspended solids concentrations (x_{TSS}) and bulk liquid temperatures (T_l).

$$p_i = a_1 + a_2\ X_{MLSS} + a_3\ T_l + a_4\ (X_{MLSS})^2 + a_5\ (X_{MLSS}\ T_l) \tag{11}$$

The identified values of all a_i parameters for all p_j coefficients are shown in Table 2 whilst the resulting polynomial curves are provided in Figure 3b. τ_w is found to increase with X_{MLSS} and decrease with temperature as a consequence of increasing bulk liquid viscosity. Under lower superficial gas velocities τ_w increases proportionally with U_{SG} whilst at higher superficial gas velocities this gradient levels off due to a decrease in τ_w^{TB} which, in turn, results from a decreasing thickness of the liquid film around the Taylor bubble. The model predicts, for a given set of inputs and parameters, rather low values of gas fractions ε between 7-14%. As Figure 3a shows, ε increases approximately linearly with U_{SG} and changes insignificantly with temperature and bulk liquid viscosity.

Table 2: Values of a_i coefficients in Equation 11 for all p_j values in Equation 10, $i = 1, \ldots, 5$, $j = 1, \ldots, 4$.

	a_1	a_2	a_3	a_4	a_5
p_1	-9.884×10^{-3}	-1.106×10^{-4}	1.256×10^{-5}	1.669×10^{-6}	-3.722×10^{-7}
p_2	4.231×10^{-2}	3.862×10^{-4}	-9.708×10^{-5}	3.378×10^{-6}	-4.288×10^{-6}
p_3	0.2627	6.695×10^{-3}	-5.703×10^{-4}	-3.598×10^{-5}	-5.445×10^{-5}
p_4	– 0.151	-2.212×10^{-3}	-4.014×10^{-4}	1.985×10^{-4}	8.685×10^{-7}

Figure 4 shows the two components of τ_w: shear stress caused by the motion of liquid slugs τ_w^{LS} and Taylor bubbles τ_w^{TB} at different operating points defined in the simulation. Whilst τ_w^{LS} depends on x_{TSS} and T_l and is in a positive almost linear relationship with U_{SG}, τ_w^{TB} is independent of x_{TSS} and T_l, is approximately 6 times larger than τ_w^{LS} and

decreases rapidly with U_{SG}. The decrease in τ_w^{TB} under higher gas velocities is caused by decreasing thickness of liquid film around the Taylor Bubble δ_L and is responsible for the curvature of $\tau_w = f(U_{SG})$ visible in Figure 3b.

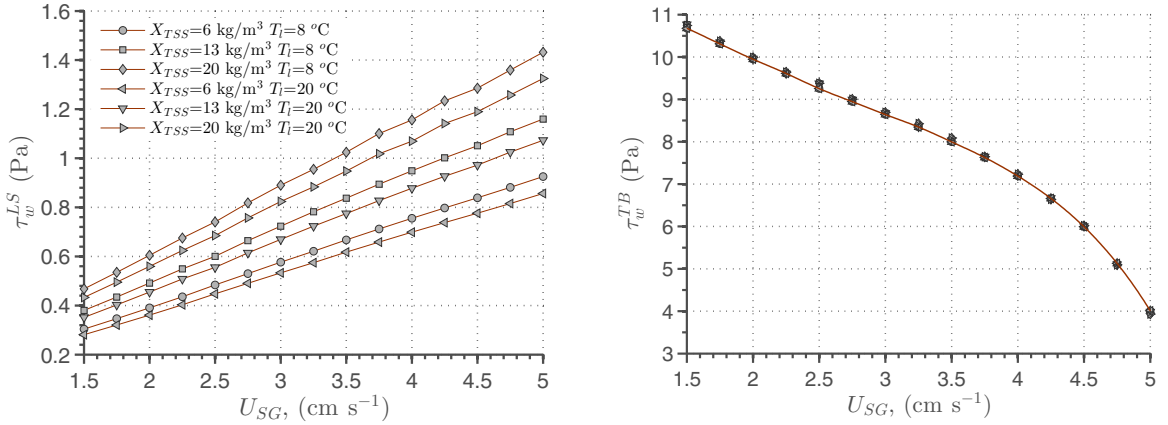

Fig. 4: Shear stresses caused by the motion of liquid slugs τ_w^{LS} and Taylor bubbles τ_w^{TB} at different superficial gas velocities U_{SG}, suspended solids concentrations x_{TSS} and bulk liquid temperatures T_l.

4. Links between biopolymer concentrations and membrane fouling

As already mentioned in Section 1 we assume that SMP are solely responsible for irreversible fouling as they deposit inside the membrane pores hence reducing the pore diameters whilst EPS lead to higher reversible fouling by reducing cake porosity. Hence, both types of biopolymers have a detrimental effect on the membrane by accelerating the overall rate of fouling. In turn, the membrane affects the bulk liquid SMP concentrations by retaining all EPS and parts of SMP within the bioreactor. Specific cake resistance, α_c changes as a function of EPS fraction in mixed liquor volatile suspended solids (MLVSS), expressed in mgTOC/gVSS, accordingly to a modified expression originally proposed by Ahmed et al.[21], shown in Equation 12. The purpose of the modification was to increase the output of the original equation of Ahmed et al.[21] as the resulting α_c values were not large enough to produce observable pressure gradients in the fouling model. Hence, both coefficients in Equation 12 are tenfold higher than in the original publication of Ahmed et al.. Although this manipulation may look dubious at first, various authors proposed different, often linear, relationships for α_c vs. EPS content in activated sludge in which the calculated α_c values differ within $2-3$ orders of magnitude. For example a linear relationship of Nuengjamnong et al.[26] predicts α_c values that are 2 orders of magnitude higher than those computed from the model of Ahmed et al. although for very small reported EPS content values that are below those produced by our activated sludge model. In the absence of reliable data we therefore assume that α_c is in a linear relationship with EPS content in the activated sludge but the exact parameter values for a particular system will need to be identified on a case-by-case basis. Since the purpose of this article is to demonstrate the MBR model as a concept, such an assumption is justifiable. COD values are converted into total organic carbon (TOC) by multiplying COD by a factor of three. MLVSS are calculated from MLSS under assumption that MLVSS/MLSS is equal to 0.7.

$$\alpha_c = 1.376 \times 10^{12} \frac{EPS}{MLVSS} - 2.564 \times 10^{13} \tag{12}$$

SMP retention on the membrane is likely to depend on a large number of factors such as pore size and shape, and pore size distribution (PSD) of the membrane pores, membrane type, composition of the dynamic layer, cake porosity, floc size distribution (FSD), zeta potential, etc. For example, Song et al.[29] experimentally found a relationship between effluent SMP concentration as a function of bulk liquid SMP concentration and sludge retention time (SRT). However, it is very likely that SRT has only an indirect effect on SMP as it was already found to affect such parameters as sludge FSD.

Since none of the above listed variables are included in our model and the mechanisms of SMP rejection on MF and UF membranes are not well understood, SMP rejection is instead described with a single parameter f_{nr} which denotes the fraction of non-retained SMP, i.e. the fraction of SMP which ends up in the permeate. This parameter is then featured in the SMP mass balance equation around the membrane as described at the end of Section 2.

5. Conclusions

This paper proposes a model structure for integrated modelling of membrane bioreactors (MBRs) for wastewater treatment. Contrary to previous integrated MBR models described in the introduction, this model structure allows to link both soluble and insoluble biopolymers produced in the bioreactor to fouling, respectively irreversible fouling and reversible fouling. These links are in agreement with the current general consensus in the scientific community that SMP is the major cause of irreversible fouling (pore constriction) whilst EPS accelerates reversible fouling (cake formation). Whilst SMP feature directly in the equation of irreversible fouling (see Janus and Ulanicki[23]), increase in EPS concentrations leads to a (linear) increase in SCR accordingly to the findings of Nuengjamnong et al.[26] and Ahmed et al.[21]. The results of slug flow modelling in the hollow fibre (HF) membrane tank with the slug flow model of Zaisha and Dukler[19] supported the experimental findings, such as of Drews et al.[27], that gas fractions in normally aerated HF membrane modules are characteristic of bubbly and cap-bubbly flow rather than slug-flow and hence, the predicted Taylor bubble lengths are very short in comparison to liquid slug lengths, suggesting formation of short cap-like air bubbles. The model also predicted that shear stresses on the membrane surface increase almost linearly with superficial gas velocity U_{SG} and therefore airflow rate for lower U_{SG} values and level off for higher U_{SG} values due to a decrease in shear stresses caused by Taylor Bubbles (τ_w^{TB}) as a result of decreasing thickness of liquid film around Taylor Bubbles. Although not shown in this paper, the model was successfully simulated and provided qualitatively appropriate results with respect of biological outputs as well as fouling, as demonstrated in Janus[16] and Janus[17]. Since the complete integrated model, i.e. combination of the interface model described here with the activated sludge model and the fouling model described respectively in Janus and Ulanicki[18] and Janus and Ulanicki[23] allow to predict the production of biopolymers under different dynamic conditions as well as the behaviour of the membrane in response to changing flux and biopolymer concentrations in the feed, it can be used for process and energy optimisation on MBR-based WWTPs.‘

References

[1] A. Fenu, G. Guglielmi, J. Jimenez, M. Spèrandio, D. Saroj, B. Lesjean, C. Brepols, C. Thoeye, I. Nopens, Activated sludge model (ASM) based modelling of membrane bioreactor (MBR) processes: A critical review with special regard to MBR specificities, Water Research 44 (2010) 4272–4294.

[2] A. Zarragoitia-González, S. Schetrite, M. Alliet, U. J.-H. ad Claire Albasi, Modelling of submerged membrane bioreactor: Conceptual study about link between activated sludge biokinetics, aeration and fouling process, Journal of Membrane Science 325 (2008) 612–624.

[3] S. G. Lu, T. Imai, M. Ukita, M. Sekine, T. Higuchi, M. Fukagawa, A model for membrane bioreactor process based on the concept of formation and degradation of soluble microbial products, Water Research 35 (2001) 2038–2048.

[4] X.-Y. Li, X.-M. Wang, Modelling of membrane fouling in a submerged membrane bioreactor, Journal of Membrane Science 278 (2006) 151–161.

[5] G. D. Bella, G. Mannina, G. Viviani, An integrated model for physical-biological wastewater organic removal in a submerged membrane bioreactor: Model development and parameter estimation, Journal of Membrane Science 322 (2008) 1–12.

[6] Y. Lee, J. Cho, Y. Seo, J. W. Lee, K.-H. Ahn, Modeling of submerged membrane bioreactor process for wastewater treatment, Desalination 146 (2002) 451–457.

[7] G. Mannina, G. di Bella, G. Viviani, An integrated model for biological and physical process simulation in membrane bioreactors (MBRs), Journal of Membrane Science 376 (2011) 56–69.

[8] T. Jiang, S. Myngheer, D. J. D. Pauw, H. Spanjers, I. Nopens, M. D. Kennedy, G. Amy, P. A. Vanrolleghem, Modelling the production and degradation of soluble microbial products (SMP) in membrane bioreactors (MBR), Water Research 42 (2008) 4955–4964.

[9] C. Suh, S. Lee, J. Cho, Investigation of the effects of membrane foulig control strategies with the integrated membrane bioreactor model, Journal of Membrane Science 429 (2013) 268–281.

[10] T. Maere, B. Verrecht, S. Moerenhout, S. Judd, I. Nopens, BSM-MBR: A benchmark simulation model to compare control and operational strategies for membrane bioreactors, Water Research 45 (2011) 2181–2190.

[11] T. Janus, B. Ulanicki, Modelling SMP and EPS formation and degradation kinetics with an extended ASM3 model, Desalination 261 (2010) 117–125.

[12] A. N. Ng, A. S. Kim, A mini-review of modeling studies on membrane bioreactor (MBR) treatment for municipal wastewaters, Desalination 212 (2007) 261–281.
[13] M. Zuthi, H. Ngo, W.S.Guo, Modelling bioprocesses and membrane foulig in membrane bioreactor (MBR): A review towards finding an integrated model framework, Bioresource Technology 122 (2012) 119–129.
[14] N. Naessens, T. Maere, I. Nopens, Critical review of membrane bioraector models - part 1: Biokinetic and filtration models, Bioresource Technology 122 (2012) 95–106.
[15] N. Naessens, T. Maere, N. Ratkovich, S. Vedantam, I. Nopens, Critical review of membrane bioreactor models - part 2: Hydrodynamic and integrated models, Bioresource Technology 122 (2012) 107–118.
[16] T. Janus, Modelling and Simulation of Membrane Bioreactors for Wastewater Treatment, Ph.D. thesis, De Montfort University, School of Engineering, Media and Sustainable Development, Leicester, UK, 2013.
[17] T. Janus, Integrated mathematical model of a {MBR} reactor including biopolymer kinetics and membrane fouling, Procedia Engineering 70 (2014) 882 – 891. 12th International Conference on Computing and Control for the Water Industry, {CCWI2013}.
[18] T. Janus, B. Ulanicki, Asm1-based activated sludge model with biopolymer kinetics for integrated simulation of membrane bioreactors for wastewater treatment, Procedia Engineering (2015). 13th International Conference on Computing and Control for the Water Industry, {CCWI2015}.
[19] M. Zaisha, A. E. Dukler, Improved hydrodynamic model of two-phase slug flow in vertical tubes, Chinese Journal of Chemical Engineering 1 (1993) 18–29.
[20] J. Busch, A. Cruse, W. Marquardt, Modeling submerged hollow-fiber membrane filtration for wastewater treatment, Journal of Membrane Science 288 (2007) 94 – 111.
[21] Z. Ahmed, J. Cho, B.-R. Lim, K.-G. Song, K.-H. Ahn, Effects of sludge retention time on membrane fouling and microbial community structure in a membrane bioreactor, Journal of Membrane Science 287 (2007) 211–218.
[22] S. Liang, L. Song, G. Tao, K. A. Kekre, H. Seah, A modeling study of fouling development in membrane bioreactors for wastewater treatment., Water Environment Research 78 (2006) 857–863.
[23] T. Janus, B. Ulanicki, A behavioural membrane fouling model for integrated simulation of membrane bioreactors for wastewater treatment, Procedia Engineering (2015). 13th International Conference on Computing and Control for the Water Industry, {CCWI2015}.
[24] N. Ratkovich, W. Horn, F. Helmus, S. Rosenberger, W. Naessens, I. Nopens, T. Bentzen, Activated sludge rheology: A critical review on data collection and modelling, Water Research 47 (2013) 463 – 482.
[25] H. Nagaoka, S. Yamanishi, A. Miya, Modeling of biofouling by extracellular polymers in a membrane separation activated sludge system, Water Science and Technology 38 (1998) 497–504.
[26] C. Nuengjamnong, J. H. Kweon, J. Cho, K.-H. Ahn, C. Polprasert, Influence of extracellular polymeric substances on membrane fouling and cleaning in a submerged membrane bioreactor, Colloid Journal 67 (2005) 392–397.
[27] A. Drews, H. Prieske, E.-L. Meyer, G. Senger, M. Kraume, Advantageous and detrimental effects of air sparging in membrane filtration: Bubble movement, exerted shear and particle classification, Desalination 250 (2010) 1083–1086.
[28] L. Böhm, A. Drews, H. Prieske, P. R. Bérubé, M. Kraume, The importance of fluid dynamics for MBR fouling mitigation, Bioresource Technology 122 (2012) 50 – 61.
[29] L. Song, S. Liang, L. Yuan, Retarded transport and accumulation of soluble microbial products in a membrane bioreactor, Journal of Environmental Engineering 133 (2007) 36–43.